Non-stripe charge order in dimerized organic conductors

Takehiko Mori*

Department of Organic and Polymeric Materials, Tokyo Institute of Technology, O-okayama, Meguro-ku, Tokyo 152-8552, Japan

(Received 24 March 2016; revised manuscript received 17 May 2016; published 2 June 2016)

This paper demonstrates charge order is important in dimerized β- and κ-phase organic conductors similar to the uniform θ- and α-phase conductors. Here the magnitude of the dimerization represents the deviation from the ideal triangular lattice in analogy with the anisotropy in the θ phase. Since the ratio of the intradimer transfer integral to the interdimer transfer integral is as large as ∼2.6, these dimerized phases lead to a dimer Mott insulator, whereas the Coulomb repulsion is closer to the triangular lattice because the ratio of the intradimer Coulomb repulsion to the interdimer Coulomb repulsion is comparatively small (∼1.7). Accordingly, in the static-limit calculation, non-stripe charge order with threefold periodicity appears between the uniform and the stripe phases, and the analogy with the θ phase suggests the first-order nature of the metal-insulator transition.

DOI: 10.1103/PhysRevB.93.245104

I. INTRODUCTION

It has been widely believed that in two-dimensional organic conductors, dimer systems, such as the κ phase, generally show the Mott insulating state, whereas uniform systems, such as the θ phase, usually exhibit a charge-order state as the insulating phase. Charge order in organic conductors has been most extensively studied in θ-phase conductors, particularly in θ-(BEDT-TTF)$_2$RbM(SCN)$_4$ [BEDT-TTF: bis(ethylenedithio)tetrathiafulvalene, M = Zn and Co] [1–4]. The NMR spectra show clear splitting, indicating two kinds of donor charges schematically represented as D^+D^0 [5–7]. The x-ray diffraction shows twofold periodicity along the "stacking" axis below the metal-insulator transition temperature at $T_{\rm MI} = 190$ K reflecting the existence of horizontal charge order [8]. The optical reflectance spectra have also indicated the presence of the horizontal stripe below $T_{\rm MI}$ [9], which is stabilized by the formation of a 1-1-0-0 pattern in the diagonal direction [10] and by the ordering of the ethylenedithio groups [11]. However, satellite spots appearing at $(1/3,k,3/4)$ and $(2/3,k,1/4)$ even at 270 K together with diffuse lines running approximately in the diagonal $(a^* + c^*)$ direction indicate the presence of non-stripe charge order in the metallic state [12]. NMR exhibits broadening above 190 K [5,7], and the dielectric constant becomes large [13]. Such a non-stripe pattern is stable because organic conductors have an approximate triangular lattice [14–16], although it also agrees with the preferred nesting vector of the Fermi surface [17]. The non-stripe state has fractional charges schematically represented as $D^+D_2^{1/4+}$ and is fairly conducting instead of the charge-ordered nature. Stability of such a state suggests the presence of fluctuating charge order in the actual system. α-(BEDT-TTF)$_2$I$_3$ has non-stripe charge order inherent in the crystal symmetry [18–20] and exhibits almost flat temperature dependence of the resistivity in the metallic state. This non-stripe charge order is also interesting as the origin of the Dirac fermions because, when the discrete C molecules are removed due to the charge order, the remaining molecules make a modified honeycomb network with hollows [20–23].

Recently, Inoue *et al.* have found an anomaly in the NMR relaxation time in a dimer conductor [24] β-(*meso*-DMBEDT-TTF)$_2$PF$_6$ [DMBEDT-TTF: dimethyl-bis(ethylenedithio)tetrathiafulvalene, Fig. 1(a)] even above $T_{\rm MI} = 90$ K [25]. This compound has an ordinary β structure where the unit-cell contains two donor molecules [Fig. 1(b)]. Below $T_{\rm MI} = 90$ K, checkerboard charge order has been established [26,27] in which a pair of charge-rich molecules is located in between the dimers ($r1$), so each dimer ($r2$) has D^+D^0 or D^0D^+ charge alternately. In this state, enhancement of the dielectric constant as well as the nonlinear conductivity have been observed [28]. Inhomogeneous mixture of the dimer Mott state and the charge order has been suggested at low temperatures from the optical spectroscopy [29]. This compound exhibits superconductivity under pressure [26,30–32], so the superconducting phase borders on the charge-order phase [33]. It is accordingly questioned why such a typical dimer system shows charge order instead of the Mott insulating state. In addition, the NMR relaxation time anomaly suggests the presence of an anomalous metallic state reminiscent of the θ phase. In order to answer these questions, here we investigate charge-order patterns of the β phase using the extended Hubbard model [14]. Surprisingly, dimerization does not destroy the charge-order states. In addition, non-stripe charge order is important similar to the nondimerized θ structure. The same logic applies to other dimer systems, such as the β' and κ phases as well as even the tetramethyltetrathiafulvalene (TMTTF) salts.

II. β PHASE

The stability of the charge-order patterns is represented by the extended Hubbard model [34,35],

$$\hat{H} = \sum_{\langle ij\rangle,\sigma} t_{ij}(c_{i\sigma}^{\dagger}c_{j\sigma} + \text{H.c.}) + U\sum_i n_{i\uparrow}n_{i\downarrow} + \sum_{\langle ij\rangle} V_{ij}n_in_j, \tag{1}$$

where $c_{i\sigma}^{\dagger}$ ($c_{i\sigma}$) is the creation (annihilation) operator of a hole with spin $\sigma(=\uparrow, \downarrow)$ at site i and $n_{i\sigma} = c_{i\sigma}^{\dagger}c_{i\sigma}$ is the number operator with $n_i = n_{i\uparrow} + n_{i\downarrow}$. U is the on-site Coulomb repulsion. t_{ij} and V_{ij} are the transfer integral and the off-site Coulomb repulsion between sites i and j, where the sum $\langle ij\rangle$ runs over nearest-neighbor pairs. Since we will

*mori.t.ae@m.titech.ac.jp

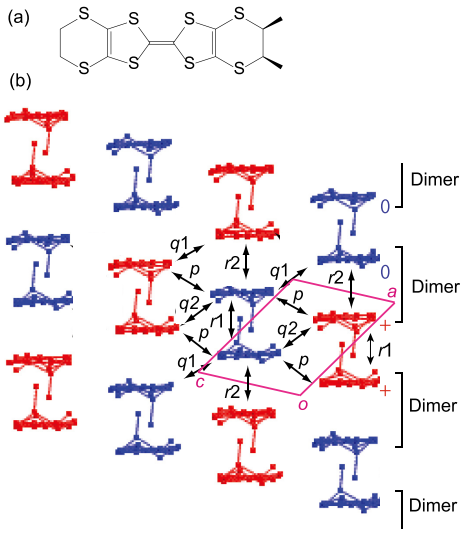

FIG. 1. (a) Molecular structure of *meso*-DMBEDT-TTF. (b) Crystal structure of β-(*meso*-DMBEDT-TTF)$_2$PF$_6$ at room temperature where the charge-order pattern below $T_{\rm MI}$ is indicated by colors. The interactions are listed in Table I.

have to investigate complicated charge-order patterns, we will neglect t_{ij} and assume the mean-field approximation (the static limit or atomic limit). Although this is a very simple model, this approximation is useful to explore various charge-order patterns that break the original lattice periodicity [14].

The network of β-(*meso*-DMBEDT-TTF)$_2$PF$_6$ is simplified as shown in Fig. 2(a). The dimers designated by the thick lines are aligned along the c axis, but without the dimerization, the intermolecular interaction makes a triangular lattice. In molecular conductors, intermolecular Coulomb repulsion V_{ij} is very well approximated by the inverse of distance R between the molecular centers [36,37]. The intermolecular distances R in β-(*meso*-DMBEDT-TTF)$_2$PF$_6$ are listed in Table I. From this, the relative magnitudes $V/V_{\rm av}$ are estimated as shown in the last column, where $V_{\rm av}$ is an average of p, $q1$, and $q2$ interactions, which corresponds to 6.68 Å. The intradimer spacing ($r2$: 3.84 Å) is short, but the interdimer interaction in the stack ($r1$: 5.67 Å) is not much different from the interstack interactions (p, $q1$, and $q2$: 6.56–6.74 Å). Then, in order to obtain the phase diagram, we will use a "V_0 approximation" in which all the latter four are approximated to be the same (V) and only the intradimer repulsion V_0 corresponding to $r2$ is larger than V. The intermolecular distance indicates $V_0/V \sim 1.74$ in the actual system.

In the uniform metal state, all n_i's are 1/2 in the mean-field approximation [Fig. 2(a)]. Without spin polarization, $n_{i\uparrow}$ and $n_{i\downarrow}$ are 1/4. Accordingly, Eq. (1) is represented by a simple analytical function of U and V as listed in Table II [14].

In the checkerboard pattern, a dimer has schematically D^+D^0 charge [Fig. 2(b)]. Since comparison of the extreme charge cases is sufficient to investigate the relative stability of charge-order patterns [36], we will use the schematic. The charge-rich pair is located on $r1$, but we can trace charge-rich molecules along the a axis as $r1$-$q1$-$r1$-$q1$. We will designate this stripe pattern as $r1$-$q1$. The checkerboard pattern is recognized as a zigzag stripe analogous to the horizontal stripe

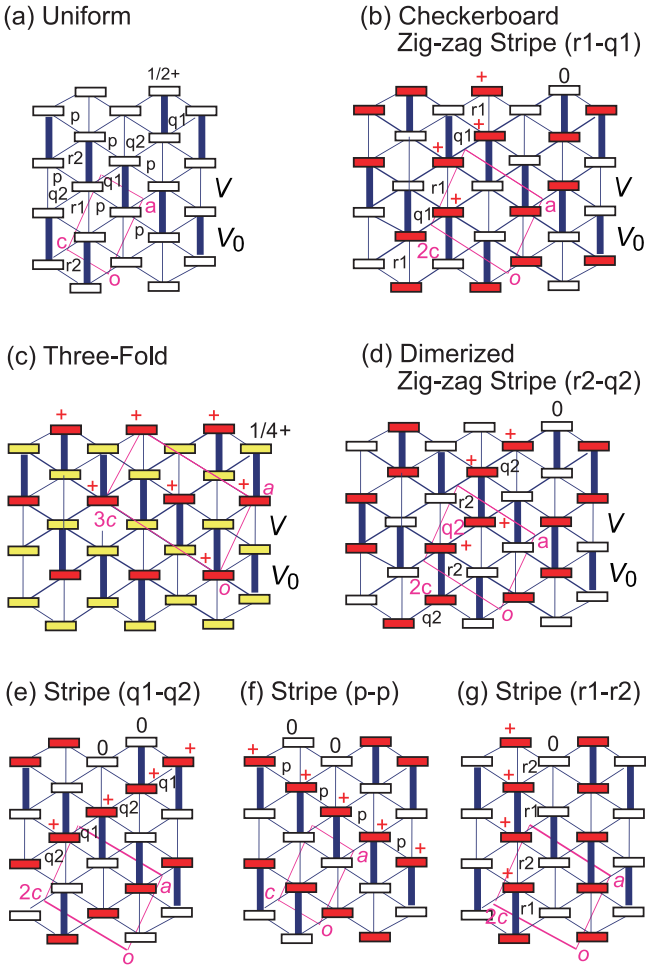

FIG. 2. Charge-order patterns of the β phase. A dimer ($r2$) is designated by a thick line. The unit-cell orientation is the same as Fig. 1(b). (a) Uniform phase, (b) checkerboard pattern (zigzag stripe along $r1$-$q1$), (c) threefold pattern, and (d) dimerized pattern (zigzag stripe along $r2$-$q2$) together with straight strips in the (e) $q1$-$q2$, (f) p-p, and (g) $r1$-$r2$ directions.

in the θ phase. Along the c axis, D^+D^0 and D^0D^+ dimers appear alternately, so the c axis is doubled. The static energy in the V_0 approximation is listed as "V_0 energy" in Table II. Similarly, "V energy" means the energy using the independent V, and "$V_{\rm av}$ energy" is the energy using the ratios $V/V_{\rm av}$ listed in Table I.

TABLE I. Transfer integrals t (meV), intermolecular distances R, and relative Coulomb repulsions $V/V_{\rm av}$ in β-(*meso*-DMBEDT-TTF)$_2$PF$_6$ [25].

Interaction	t (meV)	R (Å)	$V/V_{\rm av}$
$r1$	82.4	5.67	1.18
$r2$	226.0	3.84	1.74
p	−47.5	6.74	0.99
$q1$	43.8	6.67	1.00
$q2$	11.5	6.56	1.02

TABLE II. Energy of charge-ordered patterns per unit cell (two molecules) in the β phase.

Pattern	Charge	V_0 energy	V energy	$V_{\rm av}$ energy
Uniform	$D^{1/2+}$	$\frac{U}{8}+\frac{V_0}{4}+\frac{5V}{4}$	$\frac{U}{8}+\frac{V_{r1}+V_{r2}+V_{q1}+V_{q2}+2V_p}{4}$	$\frac{U}{8}+1.73V_{\rm av}$
Checkerboard ($r1$-$q1$)	D^+D^0	$\frac{U}{4}+V$	$\frac{U}{4}+\frac{V_{r1}+V_{q1}}{2}$	$\frac{U}{4}+1.09V_{\rm av}$
Threefold	$D^+D_2^{1/4+}$	$\frac{3U}{16}+\frac{3V_0}{16}+\frac{15V}{16}$	$\frac{3U}{16}+\frac{3(V_{r1}+V_{r2}+V_{q1}+V_{q2}+2V_p)}{16}$	$\frac{3U}{16}+1.31V_{\rm av}$
Dimerized ($r2$-$q2$)	D^+D^0	$\frac{U}{4}+\frac{V_0}{2}+\frac{V}{2}$	$\frac{U}{4}+\frac{V_{r2}+V_{q2}}{2}$	$\frac{U}{4}+1.38V_{\rm av}$
Stripe ($q1$-$q2$)	D^+D^0	$\frac{U}{4}+V$	$\frac{U}{4}+\frac{V_{q1}+V_{q2}}{2}$	$\frac{U}{4}+1.01V_{\rm av}$
Stripe (p-p)	D^+D^0	$\frac{U}{4}+V$	$\frac{U}{4}+V_p$	$\frac{U}{4}+0.99V_{\rm av}$
Stripe ($r1$-$r2$)	D^+D^0	$\frac{U}{4}+\frac{V_0}{2}+\frac{V}{2}$	$\frac{U}{4}+\frac{V_{r1}+V_{r2}}{2}$	$\frac{U}{4}+1.46V_{\rm av}$

In order to make a non-stripe pattern analogous to the θ phase, starting from a D^+ molecule, the next D^+ molecules are placed in the bisector directions of two bonds [Fig. 2(c)]. In other words, charge-rich (red) molecules are removed from the triangular lattice so as to make the remaining (yellow) molecules form a honeycomb lattice. The number of the remaining charge-poor molecules are twice as large as the charge-rich molecules, and the charge-poor molecules have $1/4+$ charge. When a dimer consists of a rich-poor pair, the next pair along the c axis has poor-poor charges, and the third pair has poor-rich charges. Then, this pattern has threefold periodicity along the c axis. The static energy is listed in Table II.

In addition to these patterns, we have to consider the dimerized pattern in which the charge-rich molecules are concentrated on a dimer [Fig. 2(d)]. This pattern appears only at $V_0 < V$. This pattern is recognized as another zigzag stripe along $r2$-$q2$-$r2$-$q2$.

When U, V_0, and V are changed, the pattern with the smallest energy is realized. The phase diagram based on the V_0 approximation is depicted in Fig. 3. When U is sufficiently large, a uniform phase is most stable. The left half of the phase diagram represents the region of $V_0 > V$, and the checkerboard pattern is stable if V_0 is comparatively large; on the left end (point A) the checkerboard is the ground state when $2V_0 > U$. Note that the dimerized pattern appears in the right half of the phase diagram at $V_0 < V$. However, the threefold phase is most stable in a large region when V_0 and V are not much different. The left end of the threefold pattern is $V_0 = 3V$, which is larger than $V_c = 2V_p$ in the θ phase [14]. Here, V_c is the interaction along the stacking axis, and V_p is the diagonal interaction in the θ phase. Then, the dimerization is not at all disadvantageous for the appearance of the non-stripe phase. Similarly, the dimerization is not seriously destructive to the checkerboard pattern. The border between the checkerboard phase and the uniform phase is $U = 2V_0$ at the left end ($V = 0$), which is smaller than the border of the horizontal stripe ($U = 4V_c$) in the θ phase. This means the horizontal pattern is twice as stable, but around the center ($V_0 = V$), the stability is nearly the same. At $V_0 = V$, the non-stripe phase exists between $U = 2V$ and $U = 6V$, and this stability range is exactly the same as the θ phase. This is because at $V_0 = V$ both the dimer and the θ models reduce to a simple triangular lattice. Although the checkerboard phase in the β phase is not as stable as the horizontal phase in the θ phase, the stability of the non-stripe phase is nearly the same as the θ phase. In the β phase, the dimerization strength (V_0/V) works similar to the anisotropy (V_c/V_p). The actual $V_0/V \sim 1.74$ expected from the intermolecular distance is larger than $V_c/V_p \sim 1.2$ [39] but still within the stability region of the non-stripe phase.

In the θ phase, we have investigated the non-stripe 2×2 and 3×4 patterns with longer periodicity [14]. The stability of a sixfold pattern, which is a dislocated diagonal stripe, has also been suggested [40]. However, we could not find stability regions of these patterns within the present approximation even including the second-nearest Coulomb interactions. These patterns do not seem to have the stability region in the present β phase.

Since the basic phase diagram is quite similar to the θ phase, we can expect similar phenomena in the β phase. The uniform phase and the non-stripe phase have larger entropy than the

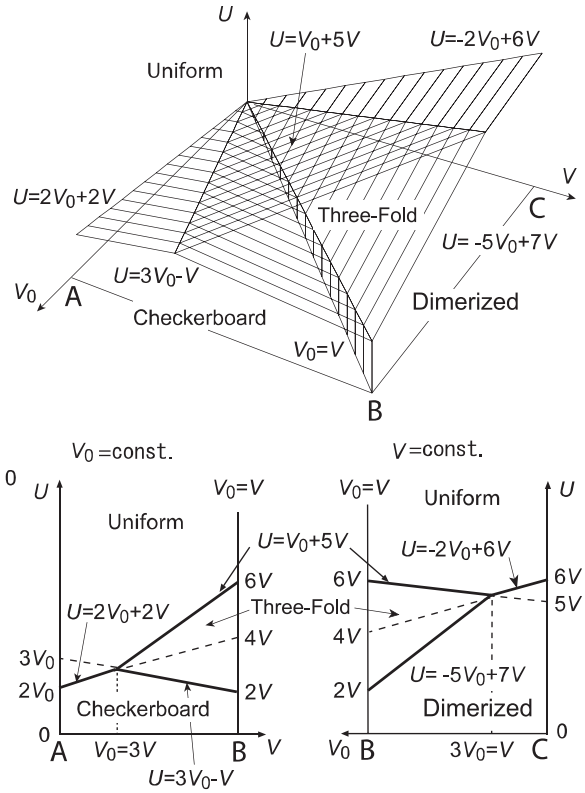

FIG. 3. Phase diagram in the V_0 approximation. The cross sections along AB and BC are depicted at the bottom.

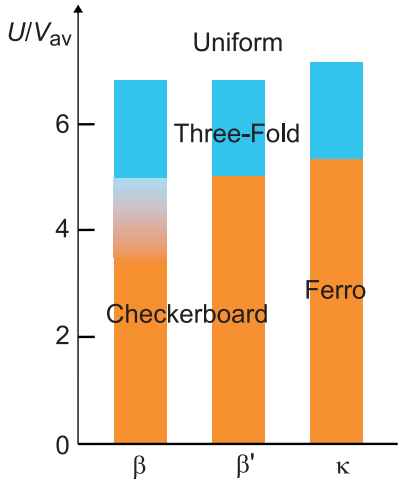

FIG. 4. Phase diagram depending on U/V_{av}.

checkerboard phase due to the fractional charges [14], and these phases become more stable at high temperatures. The finite-temperature effect has been extensively investigated on the basis of the pinball liquid model [16]. When V_0 is not larger than $3V$, the high-temperature uniform metal phase is succeeded by the non-stripe phase at low temperatures and finally replaced by the checkerboard ground state.

When V_{av} energy in Table II is compared, the pattern with the smallest V_{av} factor is most stable among the patterns with the same U factor. For patterns with different U factors, the relative stability depends on U/V_{av}, and the phase boundaries are obtained as shown in Fig. 4. This picture is in rough agreement with the properties of β-(*meso*-DMBEDT-TTF)$_2$PF$_6$. The flat temperature dependence of the resistivity at ambient pressure is consistent with the presence of the non-stripe charge order or charge fluctuation [25]. The high-temperature state has a clear optical gap below 0.18 eV [29]. The checkerboard charge order and the non-stripe charge order have different order parameters with twofold and threefold periodicities, and the transition is first order. The analogy with θ-(BEDT-TTF)$_2$CsM(SCN)$_4$ suggests a glassy mixture of these two patterns [14], in agreement with the spectroscopically observed inhomogeneity [29].

The threefold phase of the triangular lattice has been investigated by Yoshida and Hotta [16] where, instead of fractional charge ($D^{1/4+}$), double occupancy and defects are manipulated. Nonetheless, the threefold phase is stable around $V_0 \sim V$. Although a definite non-stripe charge-order pattern is assumed in the present approximation, the experimental results in the θ phase indicate this is evidence of the extraordinary stability of charge disproportionation that breaks the original lattice periodicity. The present calculation demonstrates such a state is stable not only in the θ phase, but also in the β phase.

The regular triangular lattice has three straight stripes and three zigzag stripes running in three different directions. By contrast, there is only a single kind of the threefold pattern. In order to include all possibilities, we may embed the stripes in the dimerized β pattern. The checkerboard and dimerized patterns are derived from a zigzag stripe running along the a axis [Figs. 2(b) and 2(d)]. Depending on the patterns involving and not involving the $r2$ bond, the same zigzag stripe generates two patterns: $r1$-$q1$ and $r2$-$q2$. Zigzag stripes running in the other directions make patterns with fourfold periodicity ($r1$-p-$r2$-p and $q1$-p-$q2$-p). Since these patterns do not fit the underlying β lattice, these patterns are expected to have higher energy than the simple stripes. The straight stripes make patterns along $q1$-$q2$, p-p, and $r1$-$r2$ [Figs. 2(e)–2(g)]. The $q1$-$q2$ and p-p stripes have the same energy as the checkerboard pattern in the V_0 approximation. However, V_{av} energy in Table II indicates that the $q1$-$q2$ and p-p patterns are more stable than the checkerboard ($r1$-$q1$) pattern. The stability of the actually observed checkerboard pattern is potentially related to the large $r1$ transfer and the resulting singlet formation [10,41,42]. The present approximation is probably too naive to predict the most stable state among a variety of stripe states. Nonetheless, the present calculation demonstrates the charge order is stable enough even in the nonuniform dimerized phases. The β phase has many charge-order patterns with slightly different energies, whereas the θ phase has exactly degenerated horizontal and diagonal stripes within the present approximation.

III. β' PHASE

The crystal structure of the β' phase is depicted in Fig. 5(a). The dimer interaction $a1$ (Table III) is very large, but there is no second intrastack interaction, such as $r1$ (5.67 Å), and all other interactions have intermolecular distances longer than 6.6 Å [43,44]. Therefore, the V_0 approximation is more appropriate than the β phase. The expected V_0/V is 1.74, which is about the same as the β phase. A unit cell contains a dimer as shown in Fig. 5(a). Although q or $a2$ is not strictly parallel to $a1$, the intermolecular interactions make a triangular network, which is topologically identical to the β phase. This is easily recognized as follows: Without considering the direction of the molecular planes, the bond pattern in Fig. 5(b) is a 60° rotation of Fig. 2(a). In addition to the checkerboard pattern along p-q [Fig. 5(c)] and the dimerized pattern along $a1$-$a2$ [Fig. 5(e)], the non-stripe charge order with $3c$ periodicity is possible [Fig. 5(d)]. In the V_0 approximation, the ground-state energies are the same as the β phase (Table IV), and the phase diagram is identical to Fig. 3. The phase diagram expected from V_{av} energy in Table IV is depicted in Fig. 4.

Other possibilities are straight stripes in which the charge-rich molecules align in the $a1$-q [Fig. 5(f)], $a2$-p [Fig. 5(g)], and c-c directions [Fig. 5(h)]. In the V_0 approximation, the straight stripes except for the $a1$-q pattern have the same energy as the checkerboard pattern. However, the intermolec-

TABLE III. Transfer integrals t (meV), intermolecular distances R, and relative Coulomb repulsions V/V_{av} in β'-(BEDT-TTF)$_2X$ [43,44].

Interaction	t (meV)	R (Å)	R (Å)	V/V_{av}
$a1$	264	3.85	3.83	1.74
$a2$	100	6.74	6.70	1.00
c	23	6.64	6.64	1.01
p	65	6.78	6.79	0.98
q	−20	7.44	7.61	0.88

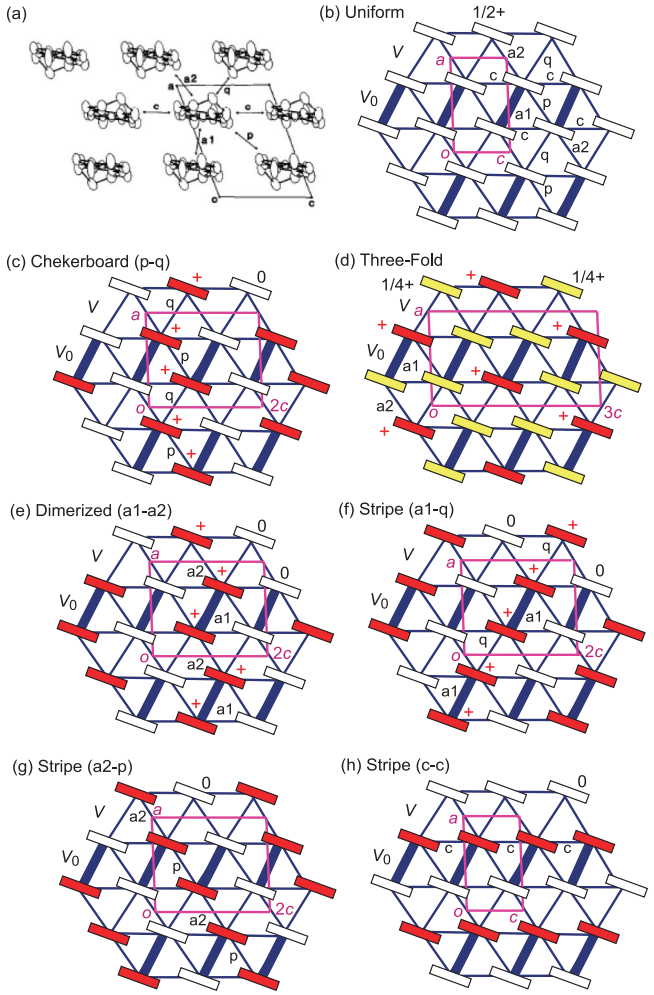

FIG. 5. (a) Crystal structure and (b) interactions in β'-(BEDT-TTF)$_2$ICl$_2$. (c) Checkerboard (p-q), (d) threefold, and (e) dimerized ($a1$-$a2$) patterns together with straight stripes in the (f) $a1$-q, (g) $a2$-p, and (f) c-c-c-c directions.

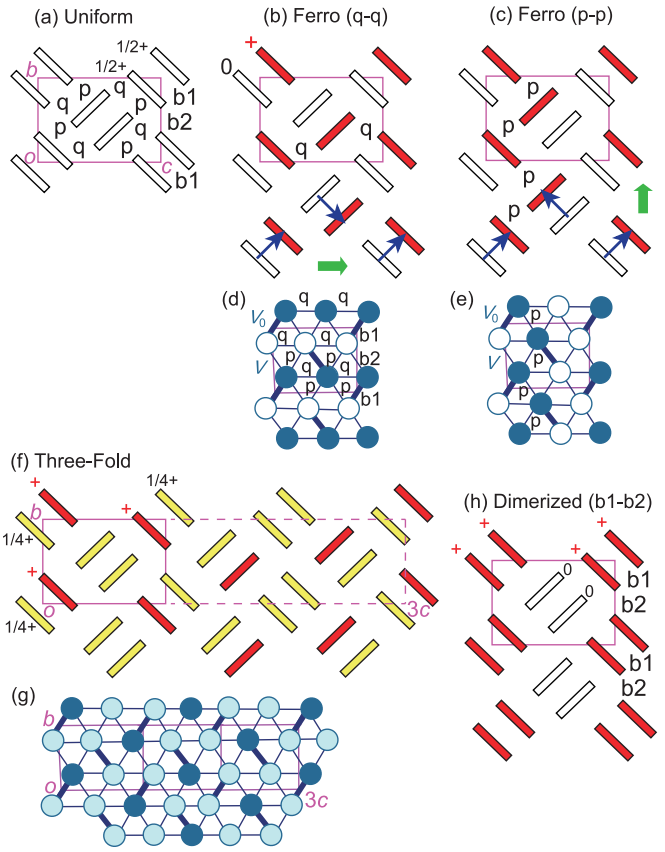

FIG. 6. (a) Uniform, (b) ferroelectric q-q, and (c) ferroelectric p-p charge-order patterns in the κ phase. The crystal lattice is that of κ-(BEDT-TTF)$_2$Cu$_2$(CN)$_3$. When the molecules are represented by circles, the network forms a triangular lattice with (d) straight (q-q), and (e) zigzag (p-p) stripes. (f) Threefold charge order and the (g) triangular network, together with the (d) dimerized ($b1$-$b2$) patterns.

ular distance q is considerably longer than $a2$, a, and p (Table III), and the zigzag p-q pattern (checkerboard) is most preferable in view of the $V_{\rm av}$ energy in Table IV.

In the β' phase, a large dielectric response has been observed around 60–100 K [45]. This has been attributed to charge disproportionation in the dimer. However, the checkerboard pattern makes a singlet state similar to the β phase. The non-stripe phase is paramagnetic and is a candidate for the dielectric anomaly because the actual β' phase is paramagnetic [46]. It should also be mentioned that the β' phase shows superconductivity at 14 K at high pressures [47].

IV. κ PHASE

Another dimer system is the κ phase. Although the κ phase has been regarded as a representative dimer Mott system, dielectric anomaly has been observed around 20 K

TABLE IV. Energy of charge-ordered patterns per unit cell (two molecules) in the β' phase.

Pattern	Charge	V_0 energy	V energy	$V_{\rm av}$ energy
Uniform	$D^{1/2+}$	$\frac{U}{8}+\frac{V_0}{4}+\frac{5V}{4}$	$\frac{U}{8}+\frac{V_{a1}+V_{a2}+V_p+V_q+2V_c}{4}$	$\frac{U}{8}+1.66V_{\rm av}$
Checkerboard (p-q)	D^+D^0	$\frac{U}{4}+V$	$\frac{U}{4}+\frac{V_p+V_q}{2}$	$\frac{U}{4}+0.93V_{\rm av}$
Threefold	$D^+D_2^{1/4+}$	$\frac{3U}{16}+\frac{3V_0}{16}+\frac{15V}{16}$	$\frac{3U}{16}+\frac{3(V_{a1}+V_{a2}+V_p+V_q+2V_c)}{16}$	$\frac{3U}{16}+1.24V_{\rm av}$
Dimerized ($a1$-$a2$)	D^+D^0	$\frac{U}{4}+\frac{V_0}{2}+\frac{V}{2}$	$\frac{U}{4}+\frac{V_{a1}+V_{a2}}{2}$	$\frac{U}{4}+1.37V_{\rm av}$
Stripe ($a1$-q)	D^+D^0	$\frac{U}{4}+\frac{V_0}{2}+\frac{V}{2}$	$\frac{U}{4}+\frac{V_{a1}+V_q}{2}$	$\frac{U}{4}+1.31V_{\rm av}$
Stripe ($a2$-p)	D^+D^0	$\frac{U}{4}+V$	$\frac{U}{4}+\frac{V_{a2}+V_p}{2}$	$\frac{U}{4}+0.99V_{\rm av}$
Stripe (c-c)	D^+D^0	$\frac{U}{4}+V$	$\frac{U}{4}+V_c$	$\frac{U}{4}+1.01V_{\rm av}$

TABLE V. Transfer integrals t (meV), the intermolecular distances R, and relative Coulomb repulsions V/V_{av} in κ-(BEDT-TTF)$_2X$ [39,64].

X = Cu[N(CN)$_2$]Cl Cu$_2$(CN)$_3$				
Interaction	t (meV)	R (Å)	R (Å)	V/V_{av}
$b1$	273	3.90	4.06	1.65
$b2$	104	6.51	6.57	1.02
p	105	5.55	5.67	1.18
q	39	6.63	6.88	0.97

in κ-(BEDT-TTF)$_2$Cu$_2$(CN)$_3$ [48]. There are considerable discussions about the origin of the anomaly [49,50], but recent observations have demonstrated the presence of some kind of charge fluctuation [51,52]. This is also the subject of intensive theoretical works [16,41,42,53–57]. Since this compound does not show an antiferromagnetic transition, this phase has been investigated as a spin-liquid system [58–61]. Recently, a similar dielectric anomaly has been found in κ-(BEDT-TTF)$_2$Cu[N(CN)$_2$]Cl [62]. This compound exhibits antiferromagnetism at 23 K [63], so it is a multiferroic system.

Intermolecular interactions in κ-(BEDT-TTF)$_2$Cu$_2$(CN)$_3$ are depicted in Fig. 6 [39,64]. Although the dimers form a triangular lattice, the network of the independent molecules is also regarded as a triangular lattice, where the $b1$ and $b2$ interactions make a zigzag arrangement along the b axis [Fig. 6(d)]. Then, dimers represented by thick lines are alternately arranged, and the tilted dimers are connected by the p and q interactions. As shown in Table V, the intradimer ($b1$) distance is short (4.06 Å), and other interactions ($b2$, p, and q) are approximated to be the same (V, Table V) in the V_0 approximation. When charge separation occurs within the dimer, there are two patterns to arrange the polarization [Figs. 6(b) and 6(c)]. The patterns in Figs. 6(b) and 6(d) are regarded as straight stripes along q-q where the charge-rich molecules are aligned in the horizontal direction. Other patterns in Figs. 6(c) and 6(e) are zigzag stripes along p-p. However, the distinction between the straight and the zigzag stripes is not essential because it comes from the idealized triangular network. Both patterns are ferroelectric, where the q-q pattern has the net polarization in the horizontal (c) direction, whereas the p-p pattern has the polarization in the vertical (b) direction. Since V_q is smaller than V_p (Table V), the q-q pattern is more stable [53]. This is also obvious from the smaller V_{av} factor in V_{av} energy in Table VI. The static energies of these uniform and charge-ordered states are calculated (Table VI), but in the V_0 approximation the results are the same as those of the β phase. The energy of the ferroelectric phase is identical to that of the checkerboard phase. This is not surprising because each molecule has six interactions in a triangular lattice, and one of the six is V_0 and the other five are V. The static energy is mostly determined by the bond numbers. The charge-rich molecules are connected uniformly along the p-p or q-q interactions so that the resulting ferroelectric phases are paramagnetic in contrast to the β-phase singlet.

Similar to the β phase, we can imagine a threefold non-stripe phase [Fig. 6(f)]. Here, the lattice is triplicated along c in which the central dimers have successively poor-poor, poor-rich, and rich-poor charges. It is obvious from the triangular lattice representation [Fig. 6(g)] that the charge-rich molecules are arranged in the bisector directions. The energy is the same as the β-phase non-stripe phase in the V_0 approximation. We have to consider another possibility, the dimerized phase [Fig. 6(d)] where the charges are preferably concentrated on a dimer. This is a zigzag stripe along $b1$-$b2$ and appears only at $V_0 < V$. Although this charge order seems unlikely, the static example has been known for a long time [65]. Then, the resulting phase diagram is identical to that of the β phase in the V_0 approximation (Fig. 3) where the ferroelectric phase replaces the checkerboard phase. The border of the ferroelectric phase is the same as the checkerboard phase, and it is not particularly destabilized by the dimerization. The phase diagram expected from V_{av} energy in Table VI is depicted in Fig. 4.

Among other possibilities, one of the three straight stripes in the original triangular lattice generates the q-q stripe, but the other two make a single kind of pattern with fourfold periodicity ($b1$-p-$b2$-p). Owing to the misfit to the underlying lattice, this pattern is not preferable. One of the zigzag patterns leads to the p-p ferroelectric pattern and the $b1$-$b2$ dimerized pattern [41], but others make a pattern with eightfold periodicity ($b1$-q-p-q-$b2$-q-p-q). This pattern is also unlikely.

The competition between the ferroelectric phase and the dimer Mott state has been investigated, and the coexisting region has been suggested as a dipolar-spin liquid [53,54]. In the limit of the large intradimer transfer t_{b1}, the dimer Mott state is stable, whereas the charge-order phase is stable when V is large [53]. It has been suggested that owing to the charge order, the interdimer magnetic interaction J is reduced in some direction, and this destabilizes the antiferromagnetic order, leading to the spin-liquid state [54]. Naively speaking, the ferroelectric pattern [Figs. 4(b) and 4(c)] makes a one-

TABLE VI. Energy of charge-ordered patterns per two molecules in the κ phase.

Pattern	Charge	V_0 energy	V energy	V_{av} energy
Uniform	$D^{1/2+}$	$\frac{U}{8}+\frac{V_0}{4}+\frac{5V}{4}$	$\frac{U}{8}+\frac{V_{b1}+V_{b2}+V_p+2V_p+2V_q}{4}$	$\frac{U}{8}+1.74V_{av}$
Ferroelectric (q-q)	D^+D^0	$\frac{U}{4}+V$	$\frac{U}{4}+V_q$	$\frac{U}{4}+0.97V_{av}$
Ferroelectric (p-p)	D^+D^0	$\frac{U}{4}+V$	$\frac{U}{4}+V_p$	$\frac{U}{4}+1.18V_{av}$
Threefold	$D^+D_2^{1/4+}$	$\frac{3U}{16}+\frac{3V_0}{16}+\frac{15V}{16}$	$\frac{3U}{16}+\frac{3(V_{b1}+V_{b2}+V_p+2V_p+2V_q)}{16}$	$\frac{3U}{16}+1.30V_{av}$
Dimerized ($b1$-$b2$)	D^+D^0	$\frac{U}{4}+\frac{V_0}{2}+\frac{V}{2}$	$\frac{U}{4}+\frac{V_{b1}+V_{b2}}{2}$	$\frac{U}{4}+1.34V_{av}$

TABLE VII. Transfer integrals t (meV), intermolecular distances R, and relative Coulomb repulsions $V/V_{\rm av}$ in $(TMTTF)_2BF_4$ [72].

Interaction[a]		t (meV)	R (Å)	$V/V_{\rm av}$
$a1$	[1/2,0,0]	195	3.91	1.89
$a2$	[−1/2,0,0]	240	3.79	1.95
b	[0,1,0]	−39	7.47	0.99
$p1$	[1/2,1,0]	21	6.67	1.10
$p2$	[−1/2,/1,0]	18	7.90	0.93

[a]Interactions are defined by approximate orientations from the original molecule located around (1/4,0,0) [72].

dimensional spin chain. Because the transition from the non-stripe phase to the ferroelectric phase is first order, we have to consider the possibility of the glasslike mixture of the two patterns in analogy with the Cs salt of the θ phase [66,67].

The actual dimerization is as large as $t_{b1}/t_{b2} \sim 2.6$ from Table V, and the system is practically regarded as a dimer Mott state [53]. By contrast, the Coulomb repulsion is closer to the triangular lattice ($V_0/V \sim 1.65$), and we have to consider the possibility of non-stripe charge order. In this connection, we have to mention κ-$(BEDT\text{-}TTF)_2Hg(SCN)_2Cl$ where charge order has been suggested below the metal-to-insulator transition at 30 K [68]. Reduced dimerization has been suggested, but charge order is compatible with the dimer Mott state.

V. TMTTF

Finally, the $(TMTTF)_2X$ salts are mentioned in which the charge order has been established [69–71]. Intermolecular interactions in $(TMTTF)_2BF_4$ are listed in Table VII [72]. The TMTTF salts are different from the β phase; it is quasi-one dimensional because the transfers in the stacks (t_{a1} and t_{a2}) are about ten times larger than the other transfers. In addition, the dimerization is small ($t_{a1} \sim t_{a2}$). However, when V_{a1} and V_{a2} are regarded as V_0, the ratio $V_0/V_{\rm av}$ is less than 2 (Table VII). The network of the V_0 approximation is equivalent to the θ phase where the numbers of the Coulomb interactions V_0 and V are 2:4. Then, the phase diagram is equivalent to the θ phase instead of Fig. 3 [14]. Since the threefold phase ends at $V_c = 2V_p$ in the phase diagram of the θ phase, the estimated $V_0/V < 2$ is close to the border. If $V_0/V > 2$, the horizontal charge order (for example, zigzag stripe $p2$-b) occurs directly and is equivalent to the ordinary one-dimensional charge order. However, $V_0/V < 2$ is significantly smaller than $t_0/t \sim 10$ (Table VII), and the possibility of the non-stripe charge order is not completely excluded where an anomalous metal state may appear in a low-temperature region just above the charge-order transition even in the $(TMTTF)_2X$ salts [73–75].

VI. SUMMARY

Charge-order patterns of dimerized organic conductors are investigated. The so-called checkerboard pattern in the β phase is regarded as a zigzag stripe analogous to the horizontal stripe in the θ phase. Here, the dimerization V_0/V works similarly to the anisotropy V_c/V_p in the θ phase, and this does not fatally destroy the charge-ordered states. The β' and the κ phases have the same phase diagram as the β phase in the V_0 approximation. This simply comes from the numbers of V_0 and V interactions (1:5) in contrast to 2:4 of V_c and V_p in the θ phase.

The uniform state of the θ phase is always a metal, but the uniform state of the dimerized phases is either a metal or a Mott insulator. Then, the Kanoda phase diagram is embedded in the uniform phase of Fig. 3 using another controlling parameter U/t [76]. The magnetism of the stripe phase depends on the parent lattice; the checkerboard pattern in the β phase is singlet due to the alternating molecular arrangement [41,42], whereas the ferroelectric phase of the κ phase is paramagnetic.

Since the dimerization of the β, β', and κ phases is as large as $t_{b1}/t_{b2} \sim 2.6$, the electronic and magnetic properties are understood from the viewpoint of a dimer Mott system. In contrast, the dimerization of the Coulomb repulsion is comparatively small ($V_0/V \sim 1.7$), and the charge order is very close to that of the uniform θ phase. This makes the non-stripe charge order universal even in the dimer systems. The analogy with the θ phase suggests that the non-stripe charge order leads to the anomalous metal state with extraordinarily large charge fluctuation [24,29]. At the same time, the transition to the stripe phase becomes first order, and we have to consider the possibility of a charge-order glass state similar to the θ phase.

ACKNOWLEDGMENTS

The author is grateful to H. Mori at the Institute for Solid State Physics, the University of Tokyo for her suggestion of the anomalous metallic state in the β phase and the two ferroelectric phases in the κ phase.

[1] K. Kuroki, Sci. Technol. Adv. Mater. **10**, 024312 (2009).
[2] T. Mori, in *Nanomaterials: From Research to Applications*, edited by H. Hosono, Y. Mishima, H. Takezoe, and K. J. D. MacKenzie (Elsevier, Amsterdam, 2006), pp. 224–261.
[3] H. Mori, S. Tanaka, and T. Mori, Phys. Rev. B **57**, 12023 (1998).
[4] H. Mori, S. Tanaka, and Y. Maruyama, Bull. Chem. Soc. Jpn. **68**, 1136 (1995).
[5] R. Chiba, H. Yamamoto, K. Hiraki, T. Takahashi, and T. Nakamura, J. Phys. Chem. Solids **62**, 389 (2001).
[6] R. Chiba, H. Yamamoto, K. Hiraki, T. Takahashi, and T. Nakamura, Synth. Met. **120**, 919 (2001).
[7] K. Miyagawa, A. Kawamoto, and K. Kanoda, Phys. Rev. B **62**, R7679 (2000).
[8] H. Mori, S. Tanaka, T. Mori, A. Kobayashi, and H. Kobayashi, Bull. Chem. Soc. Jpn. **71**, 797 (1998).
[9] H. Tajima, S. Kyoden, H. Mori, and S. Tanaka, Phys. Rev. B **62**, 9378 (2000).
[10] R. T. Clay, S. Mazumdar, and D. K. Campbell, J. Phys. Soc. Jpn. **71**, 1816 (2002).
[11] P. Alemany, J.-P. Pouget, and E. Canadell, J. Phys.: Condens. Matter **27**, 465702 (2015).
[12] M. Watanabe, Y. Noda, Y. Nogami, and H. Mori, Synth. Met. **135-136**, 665 (2003).

[13] K. Inagaki, I. Terasaki, and H. Mori, Physica B **329–333**, 1162 (2003).
[14] T. Mori, J. Phys. Soc. Jpn. **72**, 1469 (2003).
[15] J. Merino, H. Seo, and M. Ogata, Phys. Rev. B **71**, 125111 (2005).
[16] T. Yoshida and C. Hotta, Phys. Rev. B **90**, 245115 (2014).
[17] K. Kuroki, J. Phys. Soc. Jpn. **75**, 114716 (2006).
[18] T. Kakiuchi, Y. Wakabayashi, H. Sawa, T. Rakahashi, and T. Nakamura, J. Phys. Soc. Jpn. **76**, 113702 (2007).
[19] T. Mori, J. Phys. Soc. Jpn. **79**, 014703 (2010).
[20] T. Mori, J. Phys. Soc. Jpn. **82**, 034712 (2013).
[21] T. Mori, Bull. Chem. Soc. Jpn. **89** (2016).
[22] N. Tajima and K. Kajita, Sci. Technol. Adv. Mater. **10**, 024308 (2009).
[23] A. Kobayashi, S. Katayama, and Y. Suzumura, Sci. Technol. Adv. Mater. **10**, 024309 (2009).
[24] A. Inoue, H. Hashimoto, K. Miyagawa, K. Kanoda, T. Isono, A. Ueda, and H. Mori (private communication).
[25] S. Kimura, T. Maejima, H. Suzuki, R. Chiba, H. Mori, T. Kawamoto, T. Mori, H. Moriyama, Y. Nishio, and K. Kajita, Chem. Commun. 2004, 2454.
[26] S. Kimura, H. Suzuki, T. Maejima, H. Mori, J. i Yamaura, T. Kakiuchi, H. Sawa, and H. Moriyama, J. Am. Chem. Soc. **128**, 1456 (2006).
[27] M. Tanaka, K. Yamamoto, M. Uruichi, T. Yamamoto, K. Yakushi, S. Kimura, and H. Mori, J. Phys. Soc. Jpn. **77**, 024714 (2008).
[28] S. Niizeki, F. Yoshikane, K. Kohno, K. Takahashi, H. Mori, Y. Bando, T. Kawamoto, and T. Mori, J. Phys. Soc. Jpn. **77**, 073710 (2008).
[29] R. Okazaki, Y. Ikemoto, T. Moriwaki, T. Shikama, K. Takahashi, H. Mori, H. Nakaya, T. Sasaki, Y. Yasui, and I. Terasaki, Phys. Rev. Lett. **111**, 217801 (2013).
[30] N. Morinaka, K. Takahashi, R. Chiba, F. Yoshikane, S. Niizeki, M. Tanaka, K. Yakushi, M. Koeda, M. Hedo, T. Fujiwara, Y. Uwatoko, Y. Nishio, K. Kajita, and H. Mori, Phys. Rev. B **80**, 092508 (2009).
[31] T. Shikama, T. Shimokawa, S. C. Lee, T. Isono, A. Ueda, K. Takahashi, A. Nakao, R. Kumai, H. Nakano, K. Kobayashi, Y. Murakami, M. Kimata, H. Tajima, K. Matsubayashi, Y. Uwatoko, Y. Nishio, K. Kajita, and H. Mori, Crystals **2**, 1502 (2012).
[32] Y. Nishida, T. Isono, A. Ueda, and H. Mori, Eur. J. Inorg. Chem. **2014**, 3845.
[33] K. Yoshimi, M. Nakamura, and H. Mori, J. Phys. Soc. Jpn. **76**, 24706 (2007).
[34] H. Seo, J. Phys. Soc. Jpn. **69**, 805 (2000).
[35] R. H. McKenzie, J. Merino, J. B. Marston, and O. P. Sushkov, Phys. Rev. B **64**, 085109 (2001).
[36] T. Mori, Bull. Chem. Soc. Jpn. **73**, 2243 (2000).
[37] For the same reason, the interlayer Coulomb interaction is considerably smaller than the intralayer interactions because the interlayer center-to-center distance (16 Å) is significantly longer than the typical distances in Table I (6 Å). Accordingly, the interlayer Coulomb interaction is a weak perturbation, and we can concentrate on the two-dimensional patterns. However, in analogy with one-dimensional charge-density waves, we can expect that the charge-order patterns in successive layers are aligned in an antiphase manner and the three-dimensional order is attained [38].
[38] H. Kobayashi and A. Kobayashi, in *Extended Linear Chain Compounds 2*, edited by J. S. Miller (Plenum, New York, 1982), p. 259.
[39] T. Mori, Bull. Chem. Soc. Jpn. **72**, 179 (1999).
[40] M. Naka and H. Seo, J. Phys. Soc. Jpn. **83**, 053706 (2014).
[41] S. Dayal, R. T. Clay, H. Li, and S. Mazumdar, Phys. Rev. B **83**, 245106 (2011).
[42] H. Li, R. T. Clay, and S. Mazumdar, J. Phys.: Condens. Matter **22**, 272201 (2010).
[43] T. Mori and H. Inokuchi, Solid State Commun. **62**, 525 (1987).
[44] H. Kobayashi, R. Kato, A. Kobayashi, G. Saito, M. Tokumoto, H. Anzai, and T. Ishiguro, Chem. Lett. **15**, 89 (1989).
[45] S. Iguchi, S. Sasaki, N. Yoneyama, H. Taniguchi, T. Nishizaki, and T. Sasaki, Phys. Rev. B **87**, 075107 (2013).
[46] N. Yoneyama, A. Miyazaki, T. Enoki, and G. Saito, Bull. Chem. Soc. Jpn. **72**, 639 (1999).
[47] H. Taniguchi, M. Miyashita, K. Uchiyama, K. Satoh, N. Mori, H. Okamoto, K. Miyagawa, and K. Kanoda, J. Phys. Soc. Jpn. **72**, 468 (2003).
[48] M. Abdel-Jawad, I. Terasaki, T. Sasaki, N. Yoneyama, N. Kobayashi, Y. Uesu, and C. Hotta, Phys. Rev. B **82**, 125119 (2010).
[49] K. Sedlmeier, S. Elsässer, D. Neubauer, R. Beyer, D. Wu, T. Ivek, S. Tomić, J. A. Schlueter, and M. Dressel, Phys. Rev. B **86**, 245103 (2012).
[50] M. Pinterić, M. Čulo, O. Milat, M. Basletić, B. Korin-Hamzić, E. Tafra, A. Hamzić, T. Ivek, T. Peterseim, K. Miyagawa, K. Kanoda, J. A. Schlueter, M. Dressel, and S. Tomić, Phys. Rev. B **90**, 195139 (2014).
[51] K. Itoh, H. Itoh, S. Saito, I. Hosako, Y. Nakamura, H. Kishida, N. Yoneyama, T. Sasaki, S. Ishihara, and S. Iwai, Phys. Rev. B **88**, 125101 (2013).
[52] K. Yakushi, K. Yamamoto, T. Yamamoto, Y. Saito, and A. Kawamoto, J. Phys. Soc. Jpn. **84**, 084711 (2015).
[53] C. Hotta, Phys. Rev. B **82**, 241104(R) (2010).
[54] M. Naka and S. Ishihara, J. Phys. Soc. Jpn. **79**, 063707 (2010).
[55] M. Naka and S. Ishihara, J. Phys. Soc. Jpn. **82**, 023701 (2013).
[56] H. Gomi, T. Imai, A. Takahashi, and M. Aihara, Phys. Rev. B **82**, 035101 (2010).
[57] H. Gomi, M. Ikenaga, Y. Hiragi, D. Segawa, A. Takahashi, T. J. Inagaki, and M. Aihara, Phys. Rev. B **87**, 195126 (2013).
[58] Y. Shimizu, K. Miyagawa, K. Kanoda, M. Maesato, and G. Saito, Phys. Rev. Lett. **91**, 107001 (2003).
[59] S. Yamashita, Y. Nakazawa, M. Oguni, Y. Oshima, H. Nojiri, Y. Shimizu, K. Miyagawa, and K. Kanoda, Nat. Phys. **4**, 459 (2008).
[60] M. Yamashita, N. Nakata, Y. Kasahara, T. Sasaki, N. Yoneyama, N. Kobayashi, S. Fujimoto, T. Shibauchi, and Y. Matsuda, Nat. Phys. **5**, 44 (2009).
[61] K. Kanoda and R. Kato, Annu. Rev. Condens. Matter Phys. **2**, 167 (2011).
[62] P. Lunkenheimer, J. Müller, S. Krohns, F. Schrettle, A. Loidl, B. Hartmann, R. Rommel, M. de Souza, C. Hotta, J. A. Schlueter, and M. Lang, Nat. Mater. **11**, 755 (2012).
[63] K. Miyagawa, A. Kawamoto, Y. Nakazawa, and K. Kanoda, Phys. Rev. Lett. **75**, 1174 (1995).

[64] U. Geiser, H. H. Wang, K. D. Carlson, J. M. Williams, H. A. Charlier, J. E. Heindl, G. A. Yaconi, B. J. Love, M. W. Lathrop, D. L. Overmyer, J. Ren, and M. H. Whangbo, Inorg. Chem. **30**, 2586 (1991).

[65] P. Le Maguere, L. Ouahab, N. Corian, C. J. Gomez-Garcia, P. Delhaes, J. Even, and M. Bertault, Solid State Commun. **97**, 27 (1996).

[66] K. Inagaki, I. Terasaki, H. Mori, and T. Mori, J. Phys. Soc. Jpn. **73**, 3364 (2004).

[67] F. Sawano, I. Terasaki, H. Mori, T. Mori, M. Watanabe, N. Ikeda, Y. Nogami, and Y. Noda, Nature (London) **437**, 522 (2005).

[68] N. Drichko, R. Beyer, E. Rose, M. Dressel, J. A. Schlueter, S. A. Turunova, E. I. Zhilyaeva, and R. N. Lyubovskaya, Phys. Rev. B **89**, 075133 (2014).

[69] J.-P. Pouget, Crystals **2**, 466 (2012).

[70] D. S. Chow, F. Zamborszky, B. Alavi, D. J. Tantillo, A. Baur, C. A. Merlic, and S. E. Brown, Phys. Rev. Lett. **85**, 1698 (2000).

[71] P. Monceau, F. Y. Nad, and S. Brazovskii, Phys. Rev. Lett. **86**, 4080 (2001).

[72] J. L. Galigne, B. Liautard, S. Peytavin, G. Brun, M. Maurin, J. M. Fabre, E. Torreiller, and L. Giral, Acta Crystallogr. B **35**, 1129 (1979).

[73] B. Liautard, S. Peytavin, G. Brun, and M. Maurin, J. Phys. **43**, 1453 (1982).

[74] K. Mortensen, E. M. Conwell, and J. M. Fabre, Phys. Rev. B **28**, 5856 (1983).

[75] C. Coulon, S. S. P. Parkin, and R. Laversanne, Phys. Rev. B **31**, 3583 (1985).

[76] K. Kanoda, Hyperfine Interactions **104**, 235 (1997).